DETERMINATION OF DOSE EQUIVALENT INDEX AND DOSE DISTRIBUTION IN THE ROTATIONAL TISSUE EQUIVALENT SPHERE

CHONG-CHUL YOOK and SOO-YONG LEE
Dept. of Nuclear Engineering, Hanyang University,
Seoul, Korea

Abstract

The dose equivalent index and dose distribution of the rotational tissue equivalent spherical phantom were determined by exposing the incident parallel beam of photon radiation in the energy ranges 0.22-1.25 Mev.

I. Introduction

The establishment of the recommendation criteria of the ICRP for the maximum absorbed dose index (D_I) and the dose equivalent index (H_I) relating to the principal concept for the radiation protection system shall be decided from the conversion factor in accordance with the actual exposure model. However, only with the current dose equivalent conversion factors couldn't sufficiently covered all the facts of actively involved with radiation works.

Therefore, in the present study, the depth dose distribution for the photon radiations were measured from the spherical phantom of the human tissue equivalent material to meet the active condition by means of changing the speed of the phantom.

II. Experimental

The TLDs used in the present study were LiF-TLD-700, and the energy of the incident photon beams of below 147 kev were obtained from x-rays sources, and the energies of gamma-rays were obtained from Cs-137 (0.66 Mev) and Co-60 (2.66×10^{10}Bq) sources, respectively. In the case of gamma-ray sources, the distances from the source center to the center of the spherical phantom embedded with LiF-TLD-700 were 100 cm and 300 cm, and the exposure dose rates at that position were 310.15 mr/h and 110 mr/h, respectively.

The phantom used were the tissue equivalent material of 30 cm diameter, density of $1 g/cm^3$ and the composition ratio of four principal elements in soft tissue, proportioned as described by ICRU: O:0.76; C:0.11; H:0.10 and N:0.26. LiF-TLD-700 were embedded in the section of the semi-sphere phantom whose geometrical parameters are the same as shown in Table 1. The spherical phantom were dividened with two semi-spherical phantom sections that were located symmetrically both sides of the central section of the phantom.

The changes in velocity of the phantom during the radiation exposure were as the following two types: the one was a stationary state (0 rpm) that the phantom were fixed on the speed control turn table and the others were rotational states of which the phantom rotates with 7 rpm as a steady velocity and 12 rpm as a fast velocity. The later two velocities were assumed to the equivalent velocities of the actual radiation workers.

Table 1. The Geometrical Parameters of the Tissue Equivalent Semi-Sphere Phantom in Spherical Polar Coordinates.

Section A: X'_{max} = 147 mm

Depth	Z-axis (mm)	X' (mm)	θ	r	φ*
3	15.5	144.5	83.88	145.33	
6	15.5	141.5	83.75	142.35	
9	15.5	138.5	83.61	139.36	
12	15.5	135.5	83.47	136.38	
15	15.5	132.5	83.33	133.40	
20	15.5	127.5	83.07	128.44	
40	15.5	67.5	77.07	69.26	
80	15.5	47.5	71.93	49.96	
120	15.5	27.5	60.59	31.57	

Section B: X'_{max} = 141.5 mm

Depth	Z-axis (mm)	X' (mm)	θ	r	φ*
3	40.5	138.5	73.70	144.30	
6	40.5	135.5	73.76	141.42	
9	40.5	132.5	73.12	139.51	
12	40.5	129.5	72.63	135.69	
15	40.5	132.5	73.12	139.51	
20	40.5	129.5	72.63	135.69	
40	40.5	101.5	68.25	109.28	
80	40.5	61.5	56.63	73.64	
100	40.5	41.5	45.70	57.99	

Section C: X'_{max} = 131.5 mm

Depth	Z-axis (mm)	X' (mm)	θ	r	φ*
3	65.5	128.5	62.99	144.23	
6	65.5	125.5	62.44	141.56	
9	65.5	123.5	61.87	138.91	
12	65.5	119.5	61.27	136.27	
15	65.5	116.5	60.65	133.65	
20	65.5	111.5	59.57	129.32	
40	65.5	91.5	54.40	112.53	
80	65.5	51.5	38.18	83.32	
100	65.5	31.5	25.68	72.68	

Section D: X'_{max} = 117.5 mm

Depth	Z-axis (mm)	X' (mm)	θ	r	φ*
3	89	114	51.02	144.63	
6	89	111	51.28	142.27	
9	90.5	108	50.04	140.91	
12	90.5	105	49.24	138.62	
15	90.5	102	48.42	136.66	
20	90.5	97	46.99	132.66	
30	90.5	77	40.39	118.82	
80	90.5	37	22.24	97.77	

Section E: X'_{max} = 95.0 mm

Depth	Z-axis (mm)	X' (mm)	θ	r	φ*
3	114	92	38.90	146.49	
6	114	89	37.98	144.63	
9	115	86	36.79	143.6	
12	115	83	35.82	141.82	
15	115	80	34.82	140.09	
20	115	75	33.11	137.3	
40	115	55	25.56	127.47	

Section F: X'_{max} = 55 mm

Depth	Z-axis (mm)	X' (mm)	θ	r	φ*
3	139	52	20.51	148.41	
6	139	49	19.42	147.38	
9	139	46	18.31	146.41	
12	139	43	17.79	145.50	
15	139	40	16.05	144.64	
25	140	30	12.09	143.18	

X' : Radius of various depth for each section.
r : Length of radius vector from the origin of the phantom section to the point of the embedded TLDs.
θ : Zenith angle.
φ* : Azimuth angle (0°, $\pm 15^{\circ}$, $\pm 30^{\circ}$, $\pm 45^{\circ}$, $\pm 60^{\circ}$, $\pm 75^{\circ}$, $\pm 90^{\circ}$).

Each of the section (A-F) as mentioned in Table 1 were dividened appropriate volume elements in order to embedded with LiF-TLD-700, as an example, the section A were classified 132 portions according to the surface and inner part of the phantom. LiF-TLD-700 were initially given the standard annealing i.e., 16 hours at 80°C followed by 1 hour at 400°C prior to the first irradiation for different parallel beams of radiation. Thermoluminescense measurement were made using the Harshow TLD reader system Model-3000 which had been built utilizing heated nitrogen gas as the heating transfer medium.

III. Results

The results of the depth dose distribution in 30 cm diameter tissue equivalent spherical phantom with three different velocities of 0, 7 and 12 rpm for parallel beam of Co-60 and Cs-137 gamma-rays, respectively, were compared in Figures 1 and 2. As shown in the Figures 1 and 2, the distributions of the maximum absorbed dose were distributed within the depth of 10 cm from the surfaces of the phantom.

The more the phantom section reached upper portions, the more the maximum absorbed dose distribution absorbed in the deeper position of the various sections of A to E. These phenomena were occurred all the same throughout the sections, excepts for the outer section F of the phantom. Furthermore, as shown in Figure 2, the maximum absorbed dose distribution of 7 rpm were distributed approximately 10 times greater than that of 12 rpm.

According to the comparison results of the dose equivalent indices obtained by rotation of the phantom as mentioned previously with that of the MIRD-5 phantom, there were not prominent discrepancy occurred in close vicinity of 80 kev, whereas the difference of 20% were occurred in the lower energy range below 80 kev. In accordance with the aspect of the condition of the radiation dose at the phantom of this study compared with parallel and divergence beam. The difference were occurred 2.5 times about 80 kev. However the maximum value of the dose equivalent index and dose equivalent should be happened about 80 kev as shown in Figure 3.

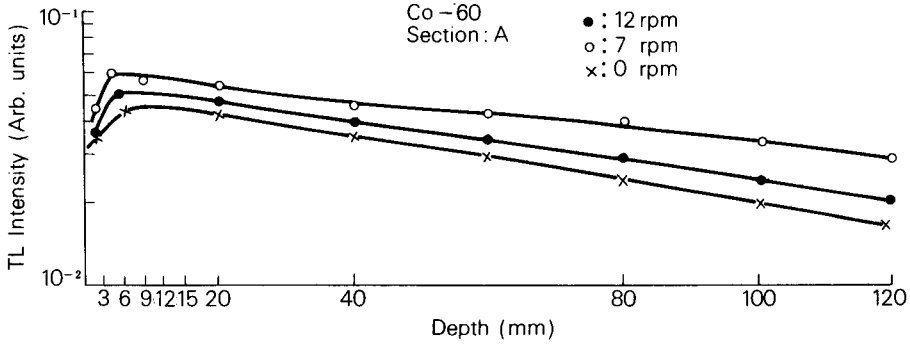

Fig. 1 Depth Dose Distribution Curves for Co-60 Gamma-Rays,

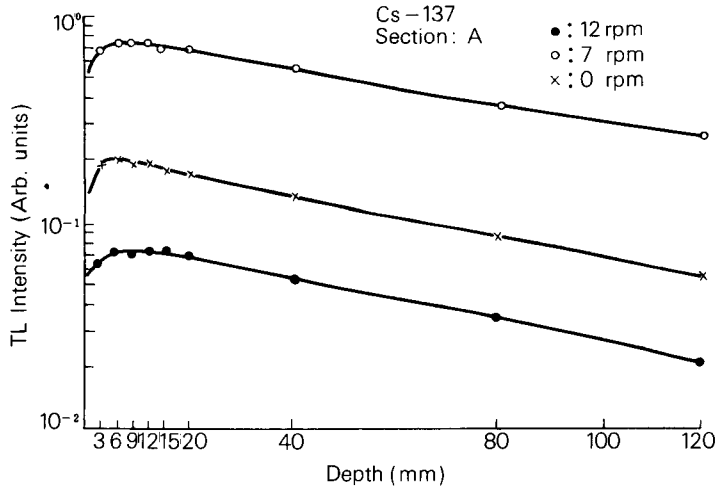

Fig. 2 Depth Dose Distribution Curves for Cs-137 Gamma-Rays.

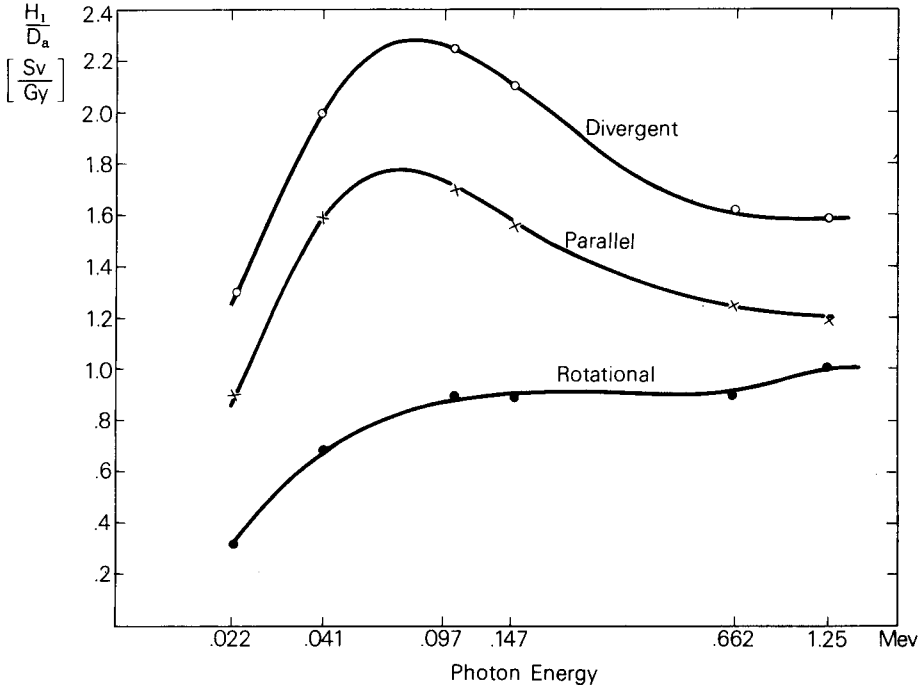

Fig. 3 Dose Equivalent Indices to the Tissue Equivalent Spherical Phantom Normalized to Absorbed Dose in Air as a Function of Photon Energy for Three Different Source Geometries.